AJEMA GLOBAL RESEARCH NETWORK

AMERICAN Journal of Engineering, Mechanics and Architecture
Volume 2, Issue 7, 2024 ISSN (E): 2993-2637

Thermal and Hydrodynamic Analysis for Micro-Pin and Micro-Channel Heat Sinks with MEPCM Present

Hind Lafta Tbena
Mechanical Engineering Department, College of Engineering, Thi-Qar University, Thi-Qar, Iraq
hindlafta88@gmail.com

Abstract: In this investigation, we used the coolant fluid, which is represented by MEPCM in MPFHS, with fins (square, triangular, and circular). Also, the Nusselt number, Reynolds numbers, and pressure drop are investigated. The MEPCM suspension uses microcapsules made from PCM (RT44) and shell materials (PAO). These capsules are immersed in pure fluids (pure oil, pure water, and ethylene glycol) at concentrations ranging from 0–20%. The results obtained reveal that MPFHS uses of MEPCM suspensions as a coolant fluid give better performance. Nessult number increased with increasing Reynolds number for all pure fluid based (RT44+PAO) suspension. Also, the variations in performance with Reynolds number for pure oil based (RT44+PAO) suspension at concentration 2%, give high performance. Because of materials properties used (RT44 and PAO), where (RT44) having a higher latent heat of fusion and PAO having a higher thermal conductivity. Furthermore, circular fins give high performance compared to square and triangular fins. Also, unfinned heat sinks give high performance compared with other types of fins due to lower pressure drop and high heat transfer coefficient.

Keywords: Micro pin fin heat sink (MPFHS), microencapsulated phase change materials (MEPCM), poly-alpha-olefin (PAO), Phase change materials (PCM).

1. Introduction

Micro-pin heat sinks are essential for cooling electronic devices because it can extract large amounts of heat from a small area. Cooling fluids, such as MEPCM suspensions, improve thermal energy storage and convection heat transfer efficiency. Several investigators have studied the presentation of heat sinks and used MEPCM.

Rami M. S. et al. (2008). The numerical study of the use of MEPCMs suspensions heat transfer in fluid to improve the efficiency of microchannel for heat sinks is currently underway. To simulate heat transfer and suspension flow, a three-dimensional symmetrical model was used. MEPCMs contain phase change materials (RT44) with a predetermined range of solidification and melting temperatures. The base receives heat flux of (100-500) W/cm2

The micro-channel heat sink measures 5.1 mm in width, 1.5 mm in height, and 10 mm in length. The heat sink micro-channel is made up of 25 rectangular channels, each measuring 100 μm wide, 500 μm deep, and 10 mm long. The results showed that, the effect of latent heat and micro-mixing caused by the use of these microencapsulated fluids improved their thermal conductivity, specific heat capacity, and effectiveness. **Tuckerman, D.B. and Pease, R.F.** (1981). Studied the effect of the liquid on the micro-channels for processor cooling, which has since been studied by numerous investigators. Micro-heat sink made from silicon to cool the water. They found that, when hydraulic diameter decreasing coefficient of heat transfer increased. Also, the researchers

successfully increased heat transfer by 40 times. **Azizi et al. (2015).** Experimentally studied of coolant fluid on the pressure drops and Nusselt number. According to their results they found that increasing the concentration of (Cu-water) nanofluid particle in microchannel leads to a higher pressure drop and Nusselt numbers. Increasing the mass fraction of nanoparticles decreased thermal resistance and increased the friction coefficient and rough Nusselt number by approximately 40% in comparison to pure water. **Anbumeenakshi, C. and Thansekhar, M.R. (2016).** Studied how the input configuration and shape of header effect on the flow distribution in micro-channels. They establish that the current distribution in a micro-channels is heavily influenced by input current, flow rate, and header shape. **Sivakumar, A. et al. (2016).** Experimental investigation of the heat transfer properties of nanofluids of CuO and Al2O3-water. The results showed that heat transfer ratios for temperatures were calculated using forced convection with nanofluids of varying particle densities. **Yang, D. et al. (2017).** A experimental and numerical study of single-phase coolant fluid function in microchannels by different pin configurations was carried out. They discovered that the shape of the pin plays an important role in balancing the heat transfer rate and pressure drop, leading to improved cooling performance. The results show that the shape of the pin fin plays a significant role in balancing pressure drop and heat transfer rate for improved cooling performance for a single- phase array's a micro channel heat sinks. **Yıldız, O. et al. (2019).** Examined the performance of graphite heat transfer containing nanofluids in an industrial microchannel. The results show that nanofluids outperform base fluids in terms of convective heat transfer coefficient. The results show that the containing graphite nanofluid has a coefficient of heat transfer that is greater than base fluids in general. Furthermore the experimental results show that the heat transfer forced convective coefficient increases with nano particles concentrations**.**

This paper numerically investigates a micro-pin fin heat sink (MPFHS) with MEPCM suspensions, including various base fluids, cores, and wall materials of microcapsules. In addition to fins, three different shapes of unfinned heat sinks are studied to analyzing the pressure drop, Nusselt number, and Reynolds numbers.

2. Geometric Configuration of Micro Pin Fins and Micro-Channel Heat Sinks

Micro-heat sink (MHS) channels have hydraulic diameters that range from 10 to 1000μm. MHSs have a high cooling capability due to single-phase fluid cooling and the large surface area of HSs over their volume, which has a higher specific heat capacity compared to air cooling. **Adeel, N. S. (2018) and Nivesh, A. M.(2013).** The term micro-pin fins heat sink (MPFHS) refers to a micro heat sink with pins that extend from its base.

Figure 1 shows the model study of micro-pin fin heat sink which have 39 fins, which have three different shapes: triangle, square, and circular. The micro-pin fin heat sink has dimensions of 20 mm in length, 100 μm in height, and 200 μm in width. The base dimensions of W_F=D_F = 25 μm and height of 75 μm for all fins and the arrangement of fins is staggered. Fin spacing: sx = 8.5 μm, sz = 8.5 μm. This model uses coupled heat transfer to generate flow. **Adeel, M. S. (2018) and Mushtaq, I. H. and Hind, L. T. (2018).**

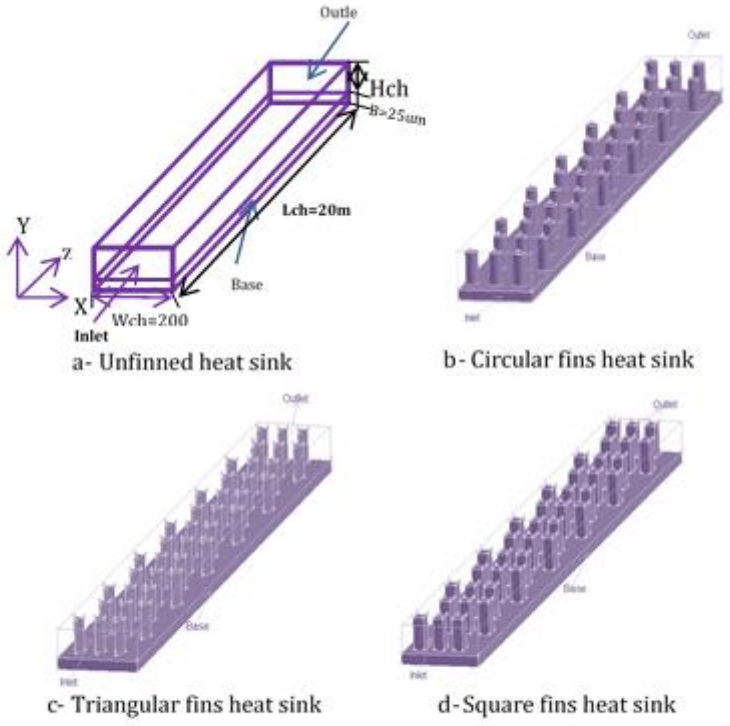

Figure 1: schematic of unfinned and finned with three types of fins (triangular, circular and square) heat sinks

3. Boundary Conditions and Governing Equations

This paper considers boundary conditions and assumptions listed below: :

A. At the wall no slip; u = v = w = 0.

B. Laminar flow, steady state flow, incompressible and heat flux applied to lower wall.

C. The top surface of micro-heat sink's is insulated.

D. The symmetry of the left and right sides of the micro-heat sink (B.C.).

E. At the channel's end fully developed flow.

F. There is no slip transfer of heat at the interface of a solid and a fluid.

The finite volume method (FVM) is used to numerically solve the system of boundary conditions and equations governing it described above. The numerical model was solved using the Computational Fluid Dynamics (CFD) model. In this study, the CFD software FLUENT 6.3 is used to solve the current model. The SIMPLE algorithm is used to compute variables related to flow and solve the velocity-pressure coupling problem. Grid size recognition is used to select an appropriate mesh for the present system's solution grid, so a mesh refinement was performed to find a suitable mesh size, yielding a highly correct answer **Nivesh, A. and Mahesh, D. (2013), Mushtaq, I. H. (2016)**.

The continuity equation:

$$\frac{\partial u}{\partial x}+\frac{\partial v}{\partial y}+\frac{\partial w}{\partial z}=0 \qquad (1)$$

Momentum equations:

$$u\frac{\partial u}{\partial x}+v\frac{\partial u}{\partial y}+w\frac{\partial u}{\partial z}=-\frac{1}{\rho}\frac{\partial \rho}{\partial x}+\frac{\mu}{\rho}\left(\frac{\partial^2 u}{\partial x^2}+\frac{\partial^2 u}{\partial y^2}+\frac{\partial^2 u}{\partial z^2}\right) \qquad (2)$$

$$u\frac{\partial v}{\partial x}+v\frac{\partial v}{\partial y}+ w\frac{\partial v}{\partial z}= -\frac{1}{\rho}\frac{\partial \rho}{\partial y}+ \frac{\mu}{\rho}(\frac{\partial^2 v}{\partial x^2}+ \frac{\partial^2 v}{\partial y^2}+ \frac{\partial^2 v}{\partial z^2}) \quad (3)$$

$$u\frac{\partial w}{\partial x}+v\frac{\partial w}{\partial y}+ w\frac{\partial w}{\partial z}= -\frac{1}{\rho}\frac{\partial \rho}{\partial z}+ \frac{\mu}{\rho}(\frac{\partial^2 w}{\partial x^2}+ \frac{\partial^2 w}{\partial y^2}+ \frac{\partial^2 w}{\partial z^2}) \quad (4)$$

Energy equation:

$$\rho Cp(u\frac{\partial He}{\partial x}+ v\frac{\partial He}{\partial y}+ w\frac{\partial He}{\partial z})= k(\frac{\partial^2 T}{\partial x^2}+ \frac{\partial^2 T}{\partial y^2}+ \frac{\partial^2 T}{\partial z^2}) \quad (5)$$

The density of PCMs was determined by calculating the mean of its liquid and solid densities from this relationship. **Nivesh, A. Mahesh, D. (2013).**

$$\rho_{PCM} = \frac{10}{7}(\frac{d_c}{d_{PCM}})^3 \rho_C \quad (6)$$

$$C_{PPCM}= \frac{(7Cpc+3\,Cpwall)\rho_c\,\rho_{wall}}{(3\,\rho c+7\,\rho wall)\rho_{PCM}} \quad (7)$$

The MEPCM particles under investigation have an average diameter of 5μm. The core elements (RT44) and shell elements (PAO) poly-alpha-olefin are investigated. The core material (PCM) in the study accounts for approximately 70% of the volume of each MEPCM particle. While the different components properties can be used to determine MEPCM requirements, the core and wall materials have distinct properties. Mass balance and energy were used separately to calculated the density and specific heat of microcapsules.

The microcapsules thermal conductivity was determined using the domain method multipart.

$$\frac{1}{K_{PCM}\,d_{PCM}} = \frac{1}{K_C\,d_c} + \frac{d_{PCM}-d_c}{K_{wall}\,d_{PCM}\,d_c} \quad (8)$$

4. Properties of Suspension

Suspension properties include fluid and microcapsule properties, and the specific heat and density of suspension are calculated using mass and energy balances.. **Mushtaq I. H. et al. (2009), Nivesh, A. and Mahesh, D. (2013).**

$$\rho_f = (1-C)\,\rho_W + C\rho_{PCM} \quad (9)$$

$$C_{PF} = (1-\varphi)\,C_{pw} + \varphi\,C_{PPCM} \quad (10)$$

The mass fraction (φ) and suspension viscosity (μ_f) were calculated employing the following mathematical calculations equations:

$$\varphi = \frac{C\rho_{PCM}}{(\rho_w+c(\rho_{PCM}-\rho_w))} = \frac{C\rho_{PCM}}{\rho_f} \quad (11)$$

$$\mu_f = \mu_w\,(1 - c - 1.16\,C^2)^{-2.5} \quad (12)$$

The relationship is functional at 20% concentration, with average component diameters between (0.3-400) μm and (20-100) the diameter-to-particle ratio **Mushtaq, I. H. et al. (2012).**

The suspension thermal conductivity (K_f) was calculated using the following equation:

$$K_f = \frac{2k_w + k_{PCM} + 2C(K_{pcm}-k_w)}{2+\frac{K_{PCM}}{k_w} - C\left(\frac{k_{PCM}}{K_w}-1\right)} \quad (13)$$

Heat sink thermal performance is determined by the rate of heat transfer and the Nusslte, Reynolds number, and Stefan numbers, which are determined by:

$$q = m \cdot C_p (T_{fin} - T_{fo}) \quad (14)$$

$$Nu = \frac{h D}{K_f} \quad (15)$$

$$Re_c = \frac{\rho u_\infty c}{\mu} \quad (16)$$

$$St = \frac{C_p T}{L} \quad (17)$$

The performance index, calculated as the heat transferred ratio (q) to the required pumping power (p.p), provides insight into the overall performance of a heat sink **Mushtaq I. H. et al. (2016).**

$$\eta = \frac{q}{p.p} \quad (18)$$

$$\text{Where: } p.p = \Delta p . V \cdot \quad (19)$$

The pressure drop is equivalent to:

$$\Delta p = p_{fout} - p_{fin} \quad (20)$$

Flow rate is equivalent to:

$$V \cdot = A . v \quad (21)$$

This study examines MEPCM suspension at the subsequent concentrations: (2, 5, 10, 15, and 20) %. Table 1 lists The physical characteristics of the materials calculated **Mushtaq, I. H. (2011).**

Table 1. The physical characteristics of suspension elements

NO Materials	ρ (kg/m3)	Cp (J/kg K)	K (W/m K)	M (kg/m s)
1 Pure-water	981.3	4189	0.643	0.000598
2 Ethylene-glycol	1111.4	2415	0.254	0.0157
3 Transformer-oil	870	2000	0.109	0.0124
4 (RT44) PCM	771	1470	0.21	_
5 (PAO) MEPCM	783	2242	0.143	_
wall				

5. Results and Discussions

5.1 Verification

The numerical model represented by **Rami, M. S. et al. (2008)** is used for validation and ensure that the model's validity. **Rami , M. S. et al. (2008)** present a numerical model of micro-channel with dimensions are: 1.5 mm vertical height, 10 mm length, and 5.1 mm width. The MEPCM volume fraction Analysis is performed on water slurry at 0% (pure water), 5%, 10%, 15%, 20%, and 25%. The temperature at the base of heat sink's was measured under certain boundary conditions. For each design model, the inlet temperature was set to 25ºC, the heat flow was retained constant at 100 W/cm2, and the bottom wall had inlet velocity of 1 m/s. To avoid

communication during validation, the results were also, Limits to pure water at a concentration of 0% and ignores rest concentrations.

Figure 2 compares the researcher Rami, M. S. et al. (2008) numerical results with the present model's temperature results along the bottom wall of heat sink's. This figure displays that when the maximum error is 0.96%, there is satisfactory arrangement between the results.

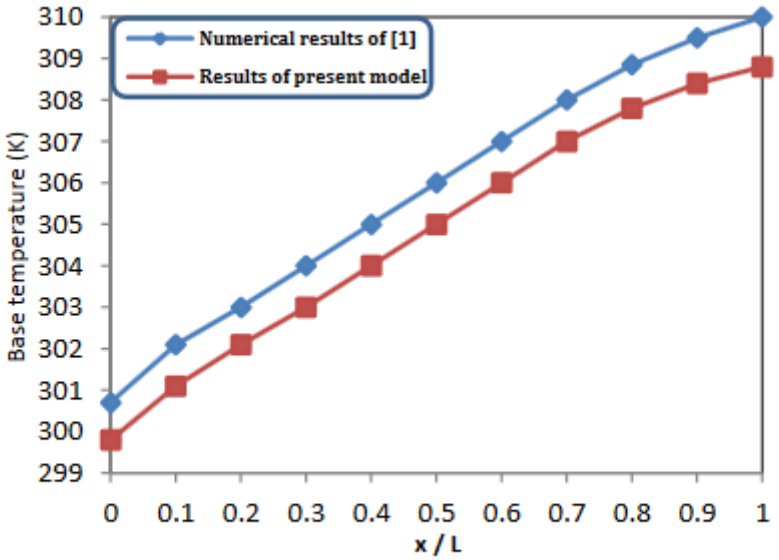

Figure 2: Change of base temperature along a micro-channel heat sink as a comparison with current model of **Rami, M. S. et al. (2008)** for pure water

5.2. Results

5.2.1 Variation of Nusslet number with Reynolds number for (pure water, ethyleneglycol, and pure oil) based (RT44+PAO) suspension at concentration 20% for unfinned and finned heat sinks:

Figures (3, 4 and 5) indicate the change of Nusslet number with Reynolds number for unfinned heat sink and finned heat sink (circular, triangular and square) for different MEPCM suspensions consists of pure fluids and different combinations of PCM and wall materials at concentration at 20%. For all figures above used MEPCM consisted for core (RT44) and MEPCM wall (PAO) for pure fluids. The boundary conditions applied for the coolants fluid (pure water, ethyleneglycol and pure oil) at constant inlet velocity (0.28 m/s), different inlet temperature and heat flux applied (640 W/m2)

The figures display that, the Nussle number increased with increasing Reynolds number due to increasing in the flow rate and inlet velocity of the heat sink. Figure 5 report that the suspension consists of (RT44) with PAO and pure oil with unfinned and finned heat sink give high Nusslet number with Reynolds number, Because of an increase in the heat transfer coefficient in the microchannel when the MEPCM slurry is used instead of pure water, as well as an increase in the slurry's heat capacity, the Nu number increases. Also, to due effects mixing caused by MEPCM because of PCM melting which has high latent heat which lead to increases the fluid heat capacity.

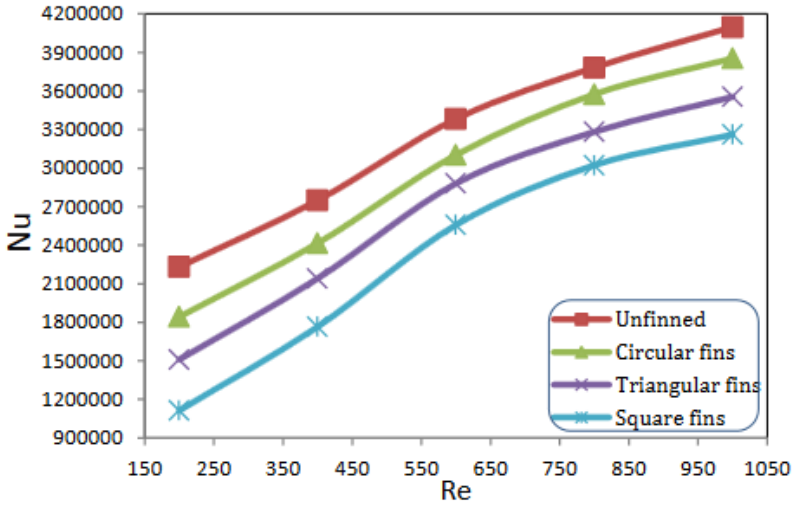

Figure 3 Variation of Nu with Reynolds number for water based (RT44+PAO) suspension at concentration 20%

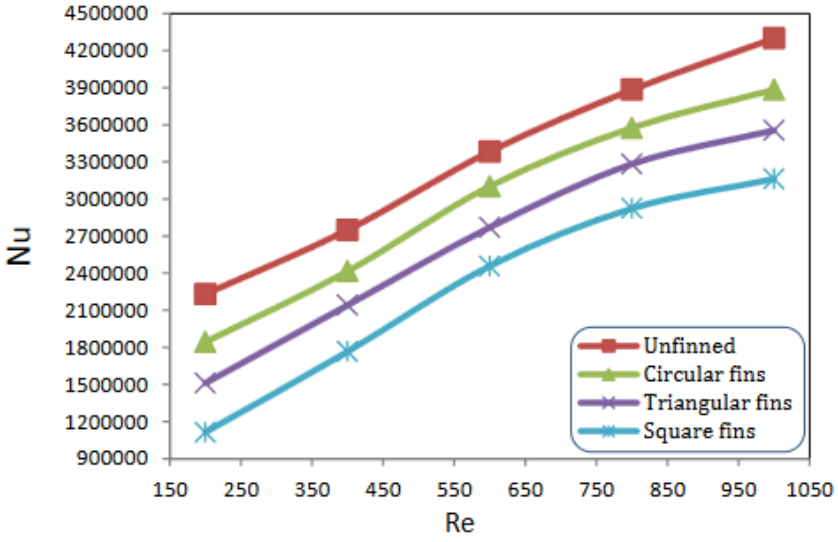

Figure 4 Variation of Nu with Reynolds number for ethyleneglycol based (RT44+PAO) suspension at concentration 20%

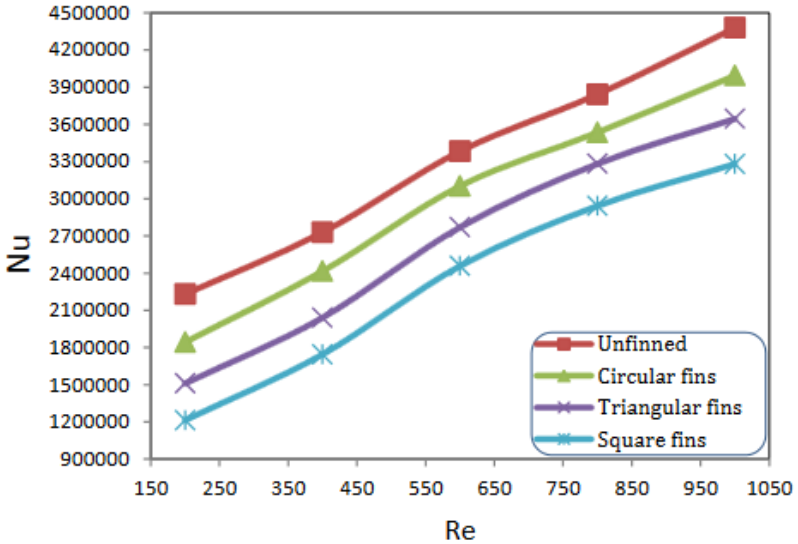

Figure 5 Variation of Nu with Reynolds number for oil based (RT44+PAO) suspension at concentration 20%

5.2.2 Variation of performance index with Reynolds number for (pure water, ethyleneglycol, and pure oil) based (RT44+PAO) suspension at concentration 2% for unfinned and finned heat sinks:

Figures (6, 7 and 8) show how the performance of heat sink varies with Reynolds number for finned (triangular, square, and circular) and unfinned heat sinks for different MEPCM suspensions containing pure fluids and various combinations of PCM and wall materials at 2% concentration for various inlet velocities. These figures show that as the Reynolds number increased, heat sink's performance decreased because of increased in pressure drop. For each of these figures, MEPCM consisted of (RT44) core and MEPCM wall (PAO) was used for pure fluid at 2% concentration because MEPCM properties increase with decreasing concentration. Figure 8 illustrate that the variations in performance with Reynolds number for pure oil based (RT44+PAO) suspension at concentration 2%, give high performance. Because of materials properties used (RT44 and PAO). Where (RT44) having a higher latent heat of fusion and PAO having a higher thermal conductivity. Furthermore, all figures show that circular fins give high performance compared to square and triangular fins. Also, unfinned heat sinks give high performance compared with other types of fins due to lower pressure drop and high heat transfer coefficient.

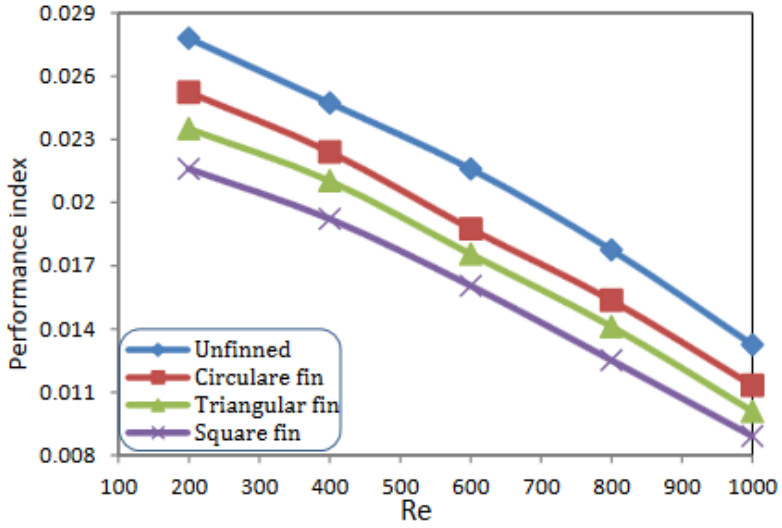

Figure 6 Variation of performance with Reynolds number for pure water based (RT44+PAO) suspension at concentration 2%

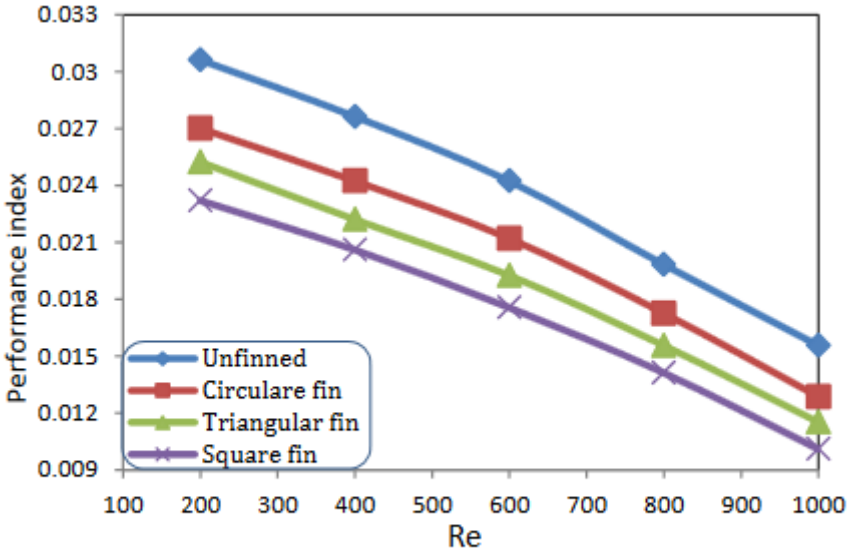

Figure 7 Variation of performance with Reynolds number for ethyleneglycol based (RT44+PAO) suspension at concentration 2%

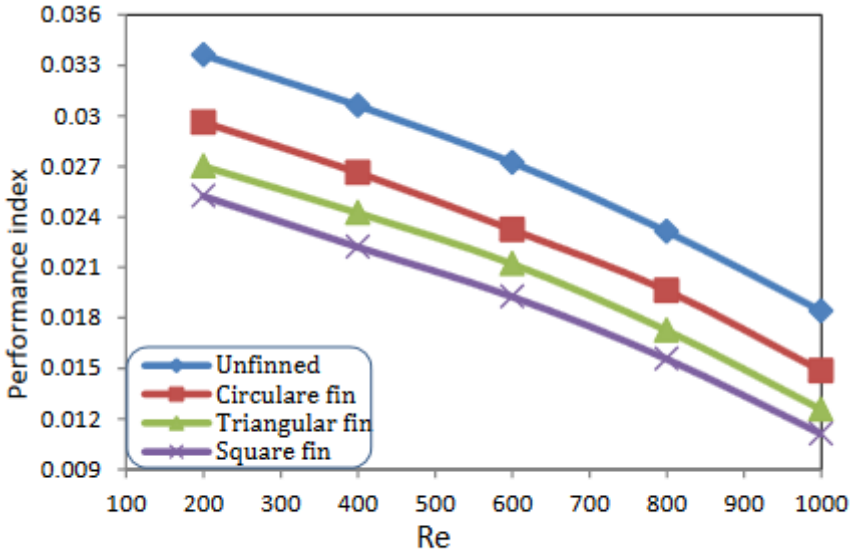

Figure 8 Variation of performance with Reynolds number for pure oil based (RT44+PAO) suspension at concentration 2%

5.2.3 The base temperature varies with stefan numbers for (pure water, ethyleneglycol, and pure oil) based (RT44+PAO) suspension at a concentration 20% for unfinned and finned heat sinks:

Figures (9, 10, and 11) show how base temperature (Θ), where Θ = ((Tb-Tin)/(Tin-Tout)) variation with the stefan number for unfinned and finned heat sinks with (square, triangular, and circular) for different MEPCM suspensions consists of pure fluids and different combinations of PCM and wall materials concentrations 20%. For all these figures, we used MEPCM suspensions consist from (RT44) core and MEPCM wall (PAO) for pure fluid. These figures demonstrated that base temperature of MEPCM suspension increased with Stefan number increasing. Due to decreased in temperature difference and amount of the heat transferred from heat sink as a results of increasing flow velocity. From figures it can be seen that, in all cases of unfinned heat sink give high temperature compared with others fins. While the circular fins give lower temperature contrasted with square and triangular fins. Because of increasing in surface exchange area and heat transfer from fins in regular shape in all directions. Also, Figure 12 gives high values of Stefan number compared with Figure 9 give low values of Stefan number due to lower value of latent heat for pure oil compared with latent heat for water.

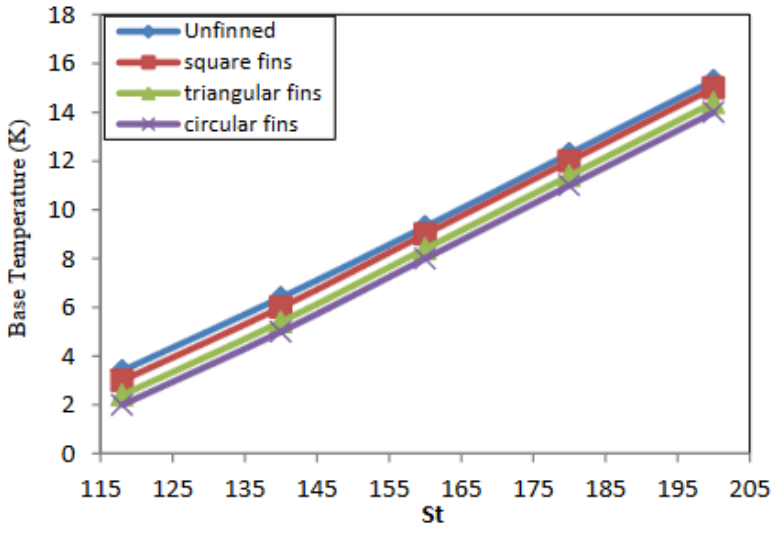

Figure 9 Variation of base temperature with Stefan number for pure water based (RT44+PAO)

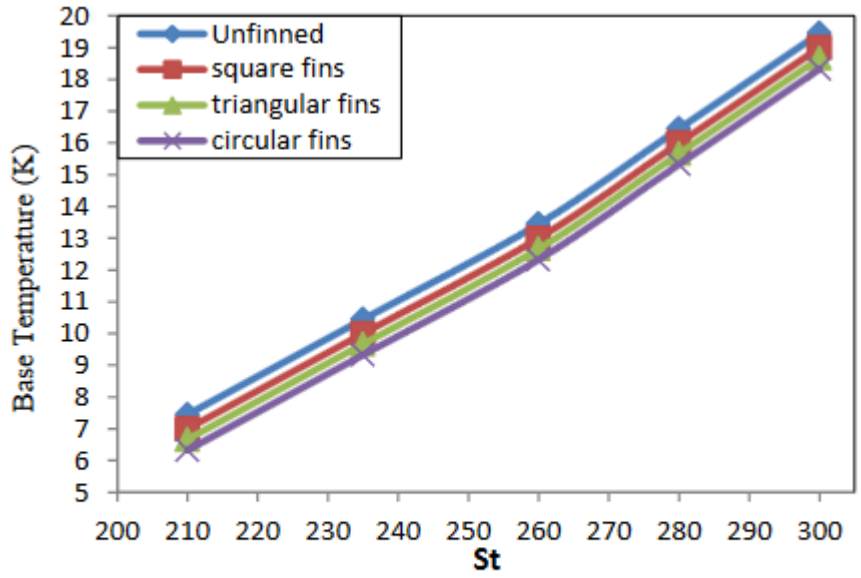

Figure 10 Variation of base temperature with Stefan number for ethyleneglycol based (RT44+PAO)

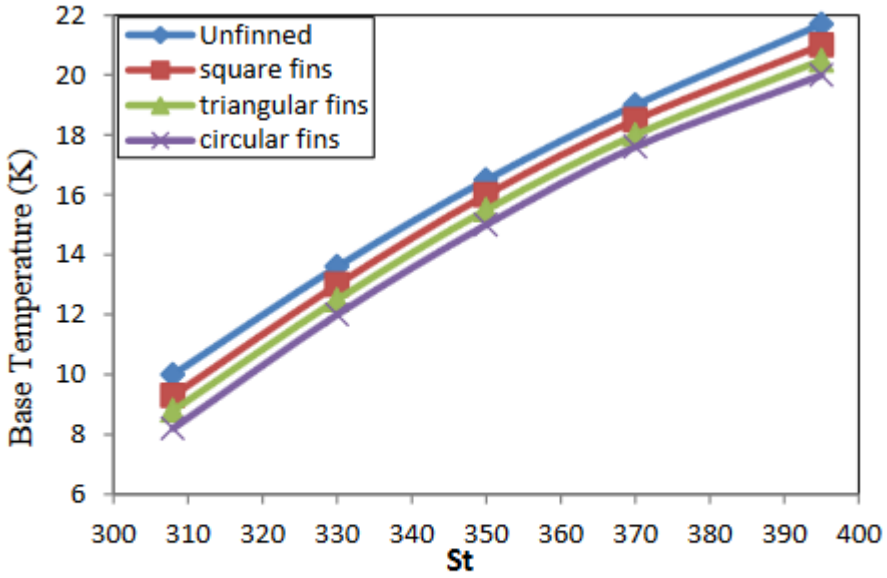

Figure 11 Variation of base temperature with Stefan number for Pure oil based (RT44+PAO)

6. Conclusions

1. As Reynolds numbers increased, Nusslet numbers increased and performance index decreased for both pure fluid and MEPCM suspension.
2. MEPCM suspension consists of pure oil and based (RT44 +PAO) suspension at a concentration 20% gives higher Nusselt number compared with all pure fluids.
3. MEPCM suspensions have been shown to improve cooling performance when used as a coolant fluid in micro-pin heat sinks instead of pure oil, ethylene glycol, or pure water.
4. Pure oil based (RT44+PAO) suspension at concentration 2o% give high base temperature with Stefan number. Due to decreased in temperature difference and amount of the heat transferred from heat sink as a results of increasing flow velocity.

7. References

1. Rami, S. Mohammed, M. and Said Al-Hallaj (2008). "Micro-channel heat sink with slurry of water with micro-encapsulated phase change material: 3D numerical study", Journal of Applied Thermal Engineering, Vol. 29, pp. 445 -454. https://doi.org/10.1016/j.applthermaleng.2008.03.027.
2. Tuckerman DB and Pease RFW, " High-performance heat sinking for VLSI", IEEE Electr Dev Lett (1981). Vol. 2, PP. 126–129, DOI:10.1109/EDL.1981.25367.
3. Azizi Z, Alamdari A and Malayeri M. (2015). "Convective heat transfer of Cu–water nanofluid in a cylindrical microchannel heat sink", Energy Convers Manag, Vol. 101, PP. 515–524, , DOI:10.1016/j.applthermaleng.2016.01.140.
4. Anbumeenakshi C and Thansekhar MR. (2016). "Experimental investigation of headed shape and inlet configuration on flow misdistribution in micro channel", Experimental and Thermal Fluid Sci, Vol. 75, PP. 156–161, DOI:10.1016/j.expthermflusci.2016.02.004
5. Sivakumar A, Alagumurthi N and Senthilvelan T. (2016) "Experimental investigation of forced convective heat transfer performance in nanofluids of Al2O3/water and CuO/water in a serpentine shaped micro channel heat sink", Heat Mass Transfer Vol. 52, PP. 1265–1274, DOI:10.1007/s00231-015-1649-5.
6. Yang D, Wang Y, Ding G, et al. (2016). "Numerical and experimental analysis of cooling performance of single-phase array microchannel heat sinks with different pin-fin configurations", Apply Thermal Eng, Vol. 112, PP. 1547–1556, DOI:10.1016/j.applthermaleng.2016.08.211.
7. Yıldız O, Ac¸ ıkgoz O, Yıldız G, et al. (2019). "Single phase flow of nanofluid including graphite and water in a microchannel", Heat Mass Transf, Vol. 56, PP. 1–24, DOI:10.1007/s00231-019-02663-5.
8. Adeel, A. Hafiz, M. Muzaffar, A. Ahmed, K. Wei-Mon, Y. Majid, A. (2018). "An experimental study of enhanced heat sinks for thermal management using n-eicosane as phase change material", Applied Thermal Engineering, Vol.132, PP. 52–66. https://doi.org/10.1016/j.applthermaleng.2017.12.066.
9. Mushtaq, I. H. and Hind, L. T. (2018). "Using of phase change materials to enhance the thermal performance of micro channel heat sink", Engineering Science and Technology, International Journal, 21, pp. 517-526. https://doi.org/10.1016/j.jestch.2018.03.017.
10. Hamza F., Abid H., Imran A., Hanzla Sh., and Hafiz M., (2022), "Experimental Analysis of Nano-Enhanced Phase-Change Material with Different Configurations of Heat Sinks", Materials (Basel), Vol.15, No.22, 8244, https://doi.org/10.3390/ma15228244.
11. Adeel, A. Hafiz, M. Muzaffar, A. Shehryar, M. (2018). " Experimental investigation of PCM based round pin-fin heat sinks for thermal management of electronics: Effect of pin-fin diameter" , International Journal of Heat and Mass Transfer, Vol. 117, PP. 861–872. https://doi.org/10.1016/j.ijheatmasstransfer.2017.10.008.
12. Nivesh, A. Mahesh, D. (2013)." Heat Transfer Analysis of Micro Channel Heat Sink", International Journal of Science and Research (IJSR), V.2, Issue1, pp.171-181, DOI:10.17577/IJERTV9IS070503.
13. Mushtaq, I. H. (2016). "Study of microchannel heat sink performance with expanded microchannels and nanofluids", Al-Qadisiyah Journal For Engineering Sciences, Vol. 9, No. 4, pp.526-542, DOI:10.1016/j.jestch.2016.03.017.
14. Mushtaq, I. H. (2011). "Numerical investigation of counter flow microchannel heat exchanger with MEPCM suspension", Applied Thermal Engineering, vol. 31, pp. 1068-1075. https://doi.org/10.1016/j.applthermaleng.2010.11.032.

15. Mushtaq, I. Abdul, A. Yaghoubi, M. Homayony, H. (2012). "Investigation of counter flow micro channel heat exchanger performance with using nanofluid as a coolant", Journal of Electronics Cooling and Thermal Control, Scientific Research, Vol. 2, pp. 35-43. DOI:10.4236/jectc.2012.23004.